Title

Label-free Optofluidic Cell Classifier Utilizing Support Vector Machines.

Authors

Wu, Tsung-Feng

Mei, Zhe

Lo, Yu-Hwa

Publication Date

2013-09-01

DOI

10.1016/j.snb.2013.06.014

Peer reviewed

Published in final edited form as:
Sens Actuators B Chem. 2013 September ; 186: 327–332. doi:10.1016/j.snb.2013.06.014.

Label-free Optofluidic Cell Classifier Utilizing Support Vector Machines

Tsung-Feng Wu[1,*], **Zhe Mei**[2,3], and **Yu-Hwa Lo**[3]

[1]Materials Science and Engineering Program at University of California at San Diego, La Jolla, CA 92093-0418 USA

[2]School of Information and Electronics, Beijing Institute of Technology, Beijing, China

[3]Department of Electrical and Computer Engineering, University of California at San Diego, La Jolla, CA 92093-0407

Abstract

A unique optofluidic lab-on-a-chip device that can measure optically encoded forward scattering signals has been demonstrated. From the design of the spatial pattern, the position and velocity of each cell in the flow can be detected and then a spatial cell distribution over the cross section of the channel can be generated. According to the forward scattering intensity and position information of cells, a data-mining method, support vector machines (SVMs), is applied for cell classification. With the help of SVMs, the multi-dimensional analysis can be performed to significantly increase all figures of merit for cell classification.

Keywords

Microfluidics; Flow cytometry; Cell classifier; Support Vector Machine (SVM); Optical-coding technique

1. Introduction

The detection and classification of biological cells with high performance tools are used for clinical diagnosis of diseases [1–7]. Today most of biomedical test instruments for cell assays are set up in hospitals or medical institutes. For large populations living in areas where such medical infrastructure is lacking, timely diagnosis and monitoring of patent conditions becomes difficult and impractical. Point-of-care is widely recognized by the global health care community as a promising approach to address the above concern. The successful implementation of the point-of-care relies on the availability of low cost, easy-to-operate, and accurate medical equipment suitable for point-of-care clinics. Lab-on-a-chip devices possess some inherent merits for point-of-care applications so have become the foci of biomedical device research. For clinical tests, samples such as blood and bodily fluids (saliva, sputum, and urine) are easy to acquire with minimum invasiveness (compared with

[*]**Corresponding author:** Tsung-Feng Wu, Materials Science and Engineering Program at University of California at San Diego, La Jolla, CA 92093-0418, USA. Tel phone: +1-858-822-2777; Fax: +1-858-534-2486; t8wu@ucsd.edu.

biopsy) and have great values in disease diagnosis and measurements of patients' health conditions. Therefore a large number of lab-on-a-chip devices for point-of-care applications are microfluidic devices for cell-based and molecular-based assays. A wide range of physical mechanisms including acoustic [8], magnetic [9], optical [10, 11] and electrical [12] effects on the biological objects have been integrated into microfluidic devices to manipulate cells and bioparticles in a similar fashion to a flow cytometer. However, most lab-on-a-chip devices today require cell labelling for cell detection, classification, and isolation from the mixture of analytes [13]. The procedures of cell labelling are usually time-consuming, hard to control, and expensive because of the high cost of reagents (e.g. fluorescently labelled anti-bodies). Also, the equipment used to detect the labelled signals is usually highly sophisticated, involving complex optics, laser sources, and sensitive photodetectors such as photomultiplier tubes (PMTs) [14]. Both the complicated and costly sample preparation procedures and the sophisticated instrument impose serious constraints on the use of such devices in point-of-care clinics. Therefore, a few groups, including ours, have moved our attention to devices that can function without cell labelling. The challenge for label-free cell-based assay is low sensitivity and specificity. Compromises in either area lead to high false positive and false negative rates, which greatly diminishes the device efficacy for point-of-care devices.

To achieve label-free cell detection and classification in high accuracy, we recently invented a method of using a spatial mask to encode the scattering signals of beads or cells in microfluidic channels [15, 16]. We demonstrated that the optical-encoding method enables us to detect forward scattering (FS) and large angle scattering (LAS) signals as well as the velocity and position of each individual cell according to its hydrodynamic behaviours governed by parameters such as cell volume, cell shape, and in particular, cell stiffness [17]. Thus without cell labelling, we have developed a method to measure many cell properties that can be used as biomarkers for cell classification (e.g. live and dead cells, red blood cells and white blood cells, subclasses of white blood cells such as lymphocytes and neutrophils).

This approach appears to be highly promising, with a demonstrated ability to detect neutropenia (low neutrophil counts) for patients undergoing chemotherapy. However, to explore the full potential of the technique for point-of-care clinics, we will need efficient cell classification algorithms to improve the detection accuracy and expand its application to more diseases and health parameters. In this article, we apply a supervised computer learning method to enhance the performance for cell classification. Support vector machine (SVM) [18–21] is one of the most powerful computer learning tools for bioinfomatics analysis. SVMs are computer-learning algorithms that use the prior knowledge to classify the unknown events. For cell classification, SVMs employ a kernel function and use existing information in the database to form a training model. After the training routine, SVMs are able to classify samples under test by their type. In addition, SVMs are able to operate in a multi-dimensional feature space to achieve higher accuracy in cell classification. Combining the SVM classification method with the encoding method of the lab-on-a-chip microfluidic device, the device performance can be significantly improved for unlabelled biological detection.

2. Materials and Methods

2.1 Design of optical-coding microfluidic devices

To optically encode forward scattering (FS) signals produced by flowing cells in a microfluidic channel, we designed a spatial mask pattern containing four transparent trapezoidal slits that allow laser to pass through for collecting scattering signals. The four-slit mask was formed by deposition and lift-off of the metal film (100 nm Ti and 200 nm Au) on a glass slide. Each trapezoidal slit has base lengths of 50 μm and 100 μm. Four slits

were alternatively arranged with a separation of 50 μm to form a 450-μm sensing area as shown in Figure 1. Depending on the pathways of particles in flow, the scattering signals of particles were encoded by the spatial mask and exhibited distinct waveforms in time domain, which were able to retrieve the space information within the microfluidic channel. The main microfluidic device with a straight channel of 5 cm in length has one inlet and one outlet. As shown in Figure 1, the microfluidic channel is with the width of 100 μm and the height of 45 μm for the entire device. The spatial mask was aligned with the microfluidic channel and placed at the downstream position of 4.5 cm from the inlet. A PIN silicon photoreceiver was optimally placed to collect the 5~10 degree FS signals. The position of particles along the direction of channel width, defined as *x*-axis, is determined by the width ratio of the first peak (*W1*) to the second peak (*W2*) of each processed event, confirmed by the width ratio of *W4* to *W3*. The velocity of particles is calculated by the total length of sensing area, 450μm, divided by the duration of passing through the pattern. Furthermore, given the channel dimensions, the position along the direction of channel height, defined as *y*-axis, can be calculated by the velocity and *x*-axis position of the particle using the characteristic parabolic velocity profile for a laminar flow within the microfluidic channel.

2.2 Theory of Support Vector Machines (SVMs)

For cell classification, the ideal scenario is to establish a classifier that divides all components into well-defined groups. However, a classifier with a clear boundary rarely exists for biological samples because of inevitable variations within the class. Increasing the dimensions of feature space can improve the performance for sample classification under such situations. One can expand those inseparable cases into a higher-dimensional feature space using the appropriate expression information. By doing so, it becomes more likely to define the hyperplane for cell classification. However, traditional learning methods in higher-dimensional feature space are usually accompanied with overfitting problems because artificially separated hyperplanes might find trivial solutions.

The algorithms of SVMs create a classifier that gives rise to a maximal margin while avoiding the overfitting problem at the same time. The simplest way for classification is to find a linear separating hyperplane, shown in Figure 2(a). Assume an expression vector x to each data point, SVMs would have a decision function $d(x,w,\mathrm{b})=w\bullet x+\mathrm{b}$, where • means dot product, w is the normal vector to the hyperplane, and b is a scalar called bias factor. Because the output of $d(x,w,\mathrm{b})$ is a scalar, the indicator function, $\boldsymbol{F}$, is defined as the sign of $d(x,w,\mathrm{b})$ that indicates which group (class) each data point belongs to. The optimal canonical hyperplane with functional margin of 1 is the contour where the decision function is equal to zero, i.e. $d(x,w,\mathrm{b})=w\bullet x+\mathrm{b}=0$, and the separating margin, γ, for both sides from the hyperplane is maximal, i.e. $2\gamma=2/\|w\|$. The principle of SVMs is to maximize the separating margin to ensure every data point is distant from the decision boundary by at least γ. After the hyperplane of SVMs is defined, an unknown vector x_{N} is classified according to the value of indication function, $\boldsymbol{F}$, defined as the sign of $d(x_{\mathrm{N}},w,\mathrm{b})$.

In general, data might not be classified linearly because of the mislabelled events in the database or inexistence of linear classifiers. The former issue can be addressed by introducing a soft margin that allows some data points to be in the wrong side of hyperplane [18]. For the latter problem, as illustrated in Figure 2 (b), a nonlinear classifier has to be defined to maximize the separating margin, by using an adequate kernel function, $K(x_i, x_j)$. Since SVM algorithms were originally based on a linear machine learning technique, introducing a nonlinear kernel function is an effective route to address the problem without changing the fundamental computation algorithms. In this case, the decision function should be substituted with the designed kernel functions that enable the SVM algorithms to achieve the nonlinear hyperplane with maximal margin. The nonlinear hyperplane is especially

important for classification in a multi-dimensional feature space, as shown in Figure 2(c). Once the analysis is conducted in n-dimensional feature space, the (n-1)-dimensional hyperplane is needed. The nonlinear kernel functions exist in various forms such as polynomial, hyperbolic tangent, inverse multi-quadratic and Gaussian radial basis function (RBF). In this article, we employ a Gaussian RBF kernel $K(x_i, x_j) = \exp(-\gamma \|x_i - x_j\|^2)$ because it has a smaller number of hyper-parameters to allow for less complex model selection and higher accuracy for our applications.

2.3 Device Fabrication and System Setup

Microfluidic devices with the designed dimensions were fabricated by curing a pre-polymer mixture comprised of polydimethylsiloxane (PDMS) (Sylgard 184, Dow Corning, MI) and a curing agent with the ratio of 10 to 1 on a silicon master which had the patterned feature using conventional soft-lithography methods. After peeling the PDMS film off from the silicon mold master, holes were punched on the PDMS replicate to create inlets and outlets of microfluidic devices. The Ti/Au film was sputtered on a cleaned glass slide to form a spatial mask by using lift-off process. After an oxygen plasma treatment, the PDMS and glass slide were bonded to form the microfluidic channels. A 488nm wavelength laser (40mW, Spectra-physics) was used as the optical source for scattering measurements. A pair of silicon photoreceivers (PDA36A, Thorlabs) was used to detect FS and LAS signals. A syringe pump (Pump 11 Elite, Harvard Apparatus, PA) was used to introduce the sample flow with the designed flux. After acquiring the scattering signals of samples, digital signal processing (DSP) was employed to filter noise and extract events. For each experiment, only one type of beads or cells was introduced into microfluidic devices for the interrogation.

To characterize optical-coding devices with selected cell types, we have prepared samples with breast cancer cells (MCF-7 cells) and white blood cells (WBCs). MCF-7 cells were cultured in the growth medium in a humidified incubator at 37°C in 5% CO_2 and then fixed with paraformaldehyde prior to the experiment. Whole blood samples used to produce WBC samples were purchased from the blood bank. To prepare WBC samples, whole blood was lysed with commercial lysing buffer (eBioscience, CA). The buffer solution used to re-suspend cells in this study consists of 10mM ethylenediaminetetraacetic acid (EDTA), 1% bovine serum albumin (BSA), and 1X phosphate buffered saline (PBS).

We trained the SVMs to recognize expression data, including FS, positions of x-axis and positions of y-axis. These factors were recorded from beads or biological cells, thus representing the true behaviours of samples flowing in the microfluidic channel. In the training procedure, two-thirds of the data were used to establish the hyperplane and the remaining one third of data were tested for the accuracy. Afterwards, we used data from several separate runs of experiment to repeatedly test the algorithm. The open source SVMs software [22] was used in the present work.

3. Results and Discussion

Using a knowledge-based algorithm to assist the classification of cells, we first trained SVMs to establish the hyperplane. To set up the database, data from MCF-7 cells and white blood cells (WBCs) were collected separately at a flow rate of 75 μL/min (Reynolds number=16.8). Figure 3(a) shows the superimposed contour plot of x-axis position versus forward scattering intensity of MCF-7 cells and WBCs. In general, MCF-7 cells have a larger diameter and produce stronger forward scattering signals than WBCs because of their larger number of scattering centers. Fluid dynamically, larger particles inside the microchannel experience a stronger lift force that drives the particles closer to the center of the microchannel [15, 23]. This lift force is given as $F_L = \rho G^2 C_L d^4$, where ρ is the density of fluid, G is the fluid shear rate ($G = 2U_f/H$), C_L is the lift coefficient (which for

microchannels remains constant when Re<100), and d is the particle diameter. As observed, the x- position of MCF-7 cells is closer to the centerline (i.e. 50μm) than the x- position of WBCs. Furthermore, due to the parabolic velocity profile within microfluidic channels, the y-position of particles can be calculated according to the parabolic relation, $\upsilon(x, y) = \upsilon_{Max}(x)\,[1-(y/h)^2]$, where $\upsilon(x, y)$ is the velocity at a specific position, $\upsilon_{Max}(x)$ is the velocity at position x and the middle of the channel (i.e., at y=0) obtained from the COMSOL simulation results, and h is the half-height of the channel, 22.5 μm in this study. Figure 3(b) and (c) shows the spatial distribution contour plots of WBCs and MCF-7 cells on the x-y plane, respectively. It is found that in the y–direction, a small yet clear separation between MCF-7 cells and WBCs is present, by a distance of 1.19 μm. This spatial separation in y-axis is attributed to different lift forces due to differences in cell size and cell stiffness. Since MCF-7 cells are larger and softer than most WBCs, both factors drive MCF-7 cells closer to the center of the channel in the y-direction [17, 24]. In the microfluidic channels, softer cells are more easily deformed into shapes that follow the streamline more closely, yielding a smaller velocity difference across the cells than stiffer cells[25]. As a result, softer cells experience a weaker drag force than stiffer cells, moving farther away from the channel wall and gaining a faster speed. In this manner, cell deformity becomes an effective biomarker for cell classification in the microfluidic channel.

The scattering signals from cells have been detected in many microfluidic devices. However, because of large variations of the signals and lack of effective methods to relate the scattering signals to the cell properties, scattering signals have not been used as a reliable method for cell classification. With the optical-coding microfluidic devices, the distribution of cells over the cross section of the microfluidic channel is explored to allow the multi-dimensional analysis by SVM analysis. Although SVMs have been widely used for bioinformatics, it is the first time the method is used to achieve accurate cell identification. SVMs can automatically create the separating boundary to classify and enumerate cells for different populations, which reduces the error by manual gating. The prediction performance of SVMs is judged by seven indicators: true positive (TP), true negative (TN), false positive (FP), false negative (FN), accuracy, sensitivity and specificity. The key figures of merit are accuracy, sensitivity and specificity defined as follow,

$$Accuracy=(TP+TN)/(TP+TN+FP+FN) \quad (1)$$

$$Sensitivity=TP/(TP+FN) \quad (2)$$

$$Specificity=TN/(FP+TN) \quad (3)$$

The outcomes of SVMs analysis are summarized in Table 1. The total events of MCF-7 cells and WBCs are 842 and 2324, respectively. For each parameter (FS, x-position, y-position), SVM analysis was performed on three separate trails. When we used FS as the only parameter for SVMs, the average values of sensitivity and accuracy are ~56.86% and 87.96%, although the specificity value (a measure of true negative rate) is very high: 99.26%.

Adding the parameter of x-axis position to the SVM analysis slightly increases the sensitivity to ~59.93%. This modest contribution suggests that although MCF-7 cells have larger FS intensity and more focused to the center position in the x-axis, these effects are insufficient for highly accurate cell classification. In contrast, adding the third parameter (y-position) to the SVMs significantly increases the accuracy and sensitivity up to 93.95% and 85.87%, respectively, while maintaining a high value of specificity (98.32%). The results

demonstrated that expanding the hyperplane to higher dimensions can significantly improve the performance for cell classification. The 2-dimensional and 3-dimensional hyperplanes are illustrated in figures 4 (a) and (b), where the hyperplane in figure 4 (b) is established using about one-third of data points for clarity in visual illustration. The minor misclassification of SVMs might result from the size variation between MCF-7 and WBCs cells, resulting unresolved parameters. However, these results still demonstrate the efficacy of SVM algorithms with optically encoded forward scattering signals from a lab-on-a-chip microfluidic device.

4. Conclusions

Forward scattering is the most common and easiest to detect signal from biological cells, but it has been a great challenge to extract biologically relevant information from the forward scattering signal alone. Our unique optical coding technique produces forward scattering signal that also contains information about cell speed and position, and such information is closely related to cell properties such as cell size, cell shape, and cell stiffness. For the first time to our knowledge, we have applied the SVMs method to perform multi-dimensional analysis of the encoded forward scattering signals. The results have shown significant enhancement in the accuracy, sensitivity, and specificity for cell classification. The encouraging initial results suggest the potential value of combining the lab-on-a-chip technology and SVMs data analysis method in point-of-care clinics.

Acknowledgments

The project described was supported by Grant Number NIH 1R43RR032225 and NIH 1R21RR024453. Its contents are solely the responsibility of the authors and do not necessarily represent the official views of the NIH.

References

1. Chin CD, Linder V, Sia SK. Lab-on-a-chip devices for global health: Past studies and future opportunities. Lab Chip. 2007; 7:41–57. [PubMed: 17180204]
2. Cline B, Kuhlmann K, Luo R. Design and Validation of a Low Cost Microscope for Diagnostics in the Developing World. Microsc Microanal. 2009; 15:870–871.
3. Mabey D, Peeling RW, Ustianowski A, Perkins MD. Diagnostics for the developing world. Nat Rev Microbiol. 2004; 2:231–240. [PubMed: 15083158]
4. Mao XL, Huang TJ. Microfluidic diagnostics for the developing world. Lab Chip. 2012; 12:1412–1416. [PubMed: 22406768]
5. Martinez AW, Phillips ST, Whitesides GM, Carrilho E. Diagnostics for the Developing World: Microfluidic Paper-Based Analytical Devices. Anal Chem. 2010; 82:3–10. [PubMed: 20000334]
6. Whitesides GM. The origins and the future of microfluidics. Nature. 2006; 442:368–373. [PubMed: 16871203]
7. Yager P, Edwards T, Fu E, Helton K, Nelson K, Tam MR, et al. Microfluidic diagnostic technologies for global public health. Nature. 2006; 442:412–418. [PubMed: 16871209]
8. Nam J, Lim H, Kim D, Shin S. Separation of platelets from whole blood using standing surface acoustic waves in a microchannel. Lab Chip. 2011; 11:3361–3364. [PubMed: 21842070]
9. Forbes TP, Forry SP. Microfluidic magnetophoretic separations of immunomagnetically labeled rare mammalian cells. Lab Chip. 2012; 12:1471–1479. [PubMed: 22395226]
10. Cho SH, Qiao W, Tsai FS, Yamashita K, Lo YH. Lab-on-a-chip flow cytometer employing color-space-time coding. Appl Phys Lett. 2010; 97
11. Dochow S, Krafft C, Neugebauer U, Bocklitz T, Henkel T, Mayer G, et al. Tumour cell identification by means of Raman spectroscopy in combination with optical traps and microfluidic environments. Lab Chip. 2011; 11:1484–1490. [PubMed: 21340095]
12. Qiao W, Cho G, Lo YH. Wirelessly powered microfluidic dielectrophoresis devices using printable RF circuits. Lab Chip. 2011; 11:1074–1080. [PubMed: 21293829]

13. Yun H, Bang H, Min J, Chung C, Chang JK, Han DC. Simultaneous counting of two subsets of leukocytes using fluorescent silica nanoparticles in a sheathless microchip flow cytometer. Lab Chip. 2010; 10:3243–3254. [PubMed: 20941407]
14. Godin J, Chen CH, Cho SH, Qiao W, Tsai F, Lo YH. Microfluidics and photonics for Bio-System-on-a-Chip: A review of advancements in technology towards a microfluidic flow cytometry chip. J Biophotonics. 2008; 1:355–376. [PubMed: 19343660]
15. Wu TF, Mei Z, Pion-Tonachini L, Zhao C, Qiao W, Arianpour A, et al. An optical-coding method to measure particle distribution in microfluidic devices. Aip Adv. 2011; 1
16. Mei Z, Wu TF, Pion-Tonachini L, Qiao W, Zhao C, Liu ZW, et al. Applying an optical space-time coding method to enhance light scattering signals in microfluidic devices. Biomicrofluidics. 2011; 5
17. Wu TF, Mei Z, Lo YH. Optofluidic device for label-free cell classification from whole blood. Lab Chip. 2012; 12:3791–3797. [PubMed: 22875178]
18. Wang, L. Support Vector Machines: theory and applications. Springer; 2005.
19. Brown MPS, Grundy WN, Lin D, Cristianini N, Sugnet CW, Furey TS, et al. Knowledge-based analysis of microarray gene expression data by using support vector machines. P Natl Acad Sci USA. 2000; 97:262–267.
20. Ramaswamy S, Tamayo P, Rifkin R, Mukherjee S, Yeang CH, Angelo M, et al. Multiclass cancer diagnosis using tumor gene expression signatures. P Natl Acad Sci USA. 2001; 98:15149–15154.
21. Furey TS, Cristianini N, Duffy N, Bednarski DW, Schummer M, Haussler D. Support vector machine classification and validation of cancer tissue samples using microarray expression data. Bioinformatics. 2000; 16:906–914. [PubMed: 11120680]
22. Chang C-JLC. LIBSVM: a library for support vector machines. ACM Transactions on Intelligent Systems and Technology. 2011 2:27:1.
23. Hur SC, Tse HTK, Di Carlo D. Sheathless inertial cell ordering for extreme throughput flow cytometry. Lab Chip. 2010; 10:274–280. [PubMed: 20090998]
24. Hur SC, Henderson-MacLennan NK, McCabe ERB, Di Carlo D. Deformability-based cell classification and enrichment using inertial microfluidics. Lab Chip. 2011; 11:912–920. [PubMed: 21271000]
25. Mortazavi S, Tryggvason G. A numerical study of the motion of drops in Poiseuille flow. Part 1. Lateral migration of one drop. J Fluid Mech. 2000; 411:325–350.

Biographies

Tsung-Feng Wu is a Ph.D. candidate at materials science and engineering program at University of California at San Diego, CA (USA). His research interests are in the field of BioMEMS, optofluidics and biomedical applications.

Zhe Mei is a Ph.D. student at the School of Information and Electronics at Beijing Institute of Technology, Beijing, China. He is also now a visiting scholar in the Department of Electrical and Computer Engineering, University of California at San Diego, CA, USA.

Yu-Hwa Lo is the professor at the Department of Electrical and Computer Engineering, University of California at San Diego, CA (USA). Currently his research interests are in bio-imaging, bio-sensing, nano-photonics, and single-photon detectors.

Highlight

Point-of-care is widely recognized by the global health care community as a promising approach to address the above concern. The successful implementation of the point-of-care relies on the availability of low cost, easy-to-operate, and accurate medical equipment suitable for point-of-care clinics. To address these issues, we demonstrated an optical-coding microfluidic device combined with the supporting vector machines (SVMs) for clinical in-vitro diagnosis. In this study, breast cancer cells (MCF-7) and human white blood cells are used to demonstrate the capability of our system. With the help of SVMs, the multi-dimensional analysis can be performed to significantly increase all figures of merit for cell classification. We show marked improvements in the performance of cell classification, measured by the rates of sensitivity (85.87%), specificity (98.32%), and accuracy (93.95%).

Highlights

- An optical-coding microfluidic device combined with the supporting vector machines (SVMs) for clinical in-vitro diagnosis is demonstrated.
- With the help of SVMs, multi-dimensional analysis is performed to enhance the cell identification.
- Breast cancer cells and human white blood cells are used to demonstrate the capability of our system.
- Significant improvements in the performance of cell classification, measured by the rates of sensitivity, specificity, and accuracy, are shown.

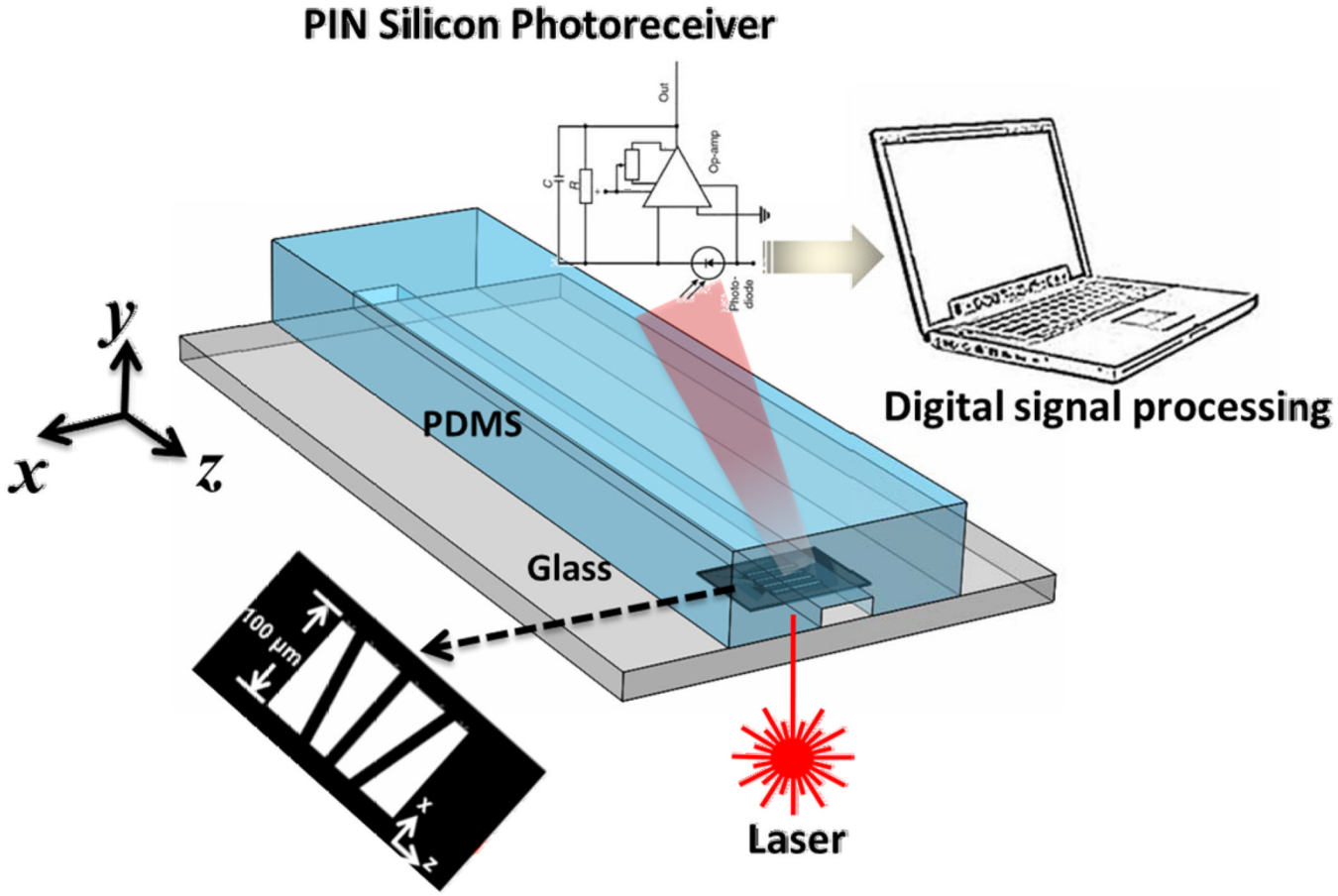

Figure 1.
A scheme of the optical-coding microfluidic channel. The beads or cells are interrogated with a laser source. The laser light is encoded after passing through the sensing area to provide the position information of beads or cells.

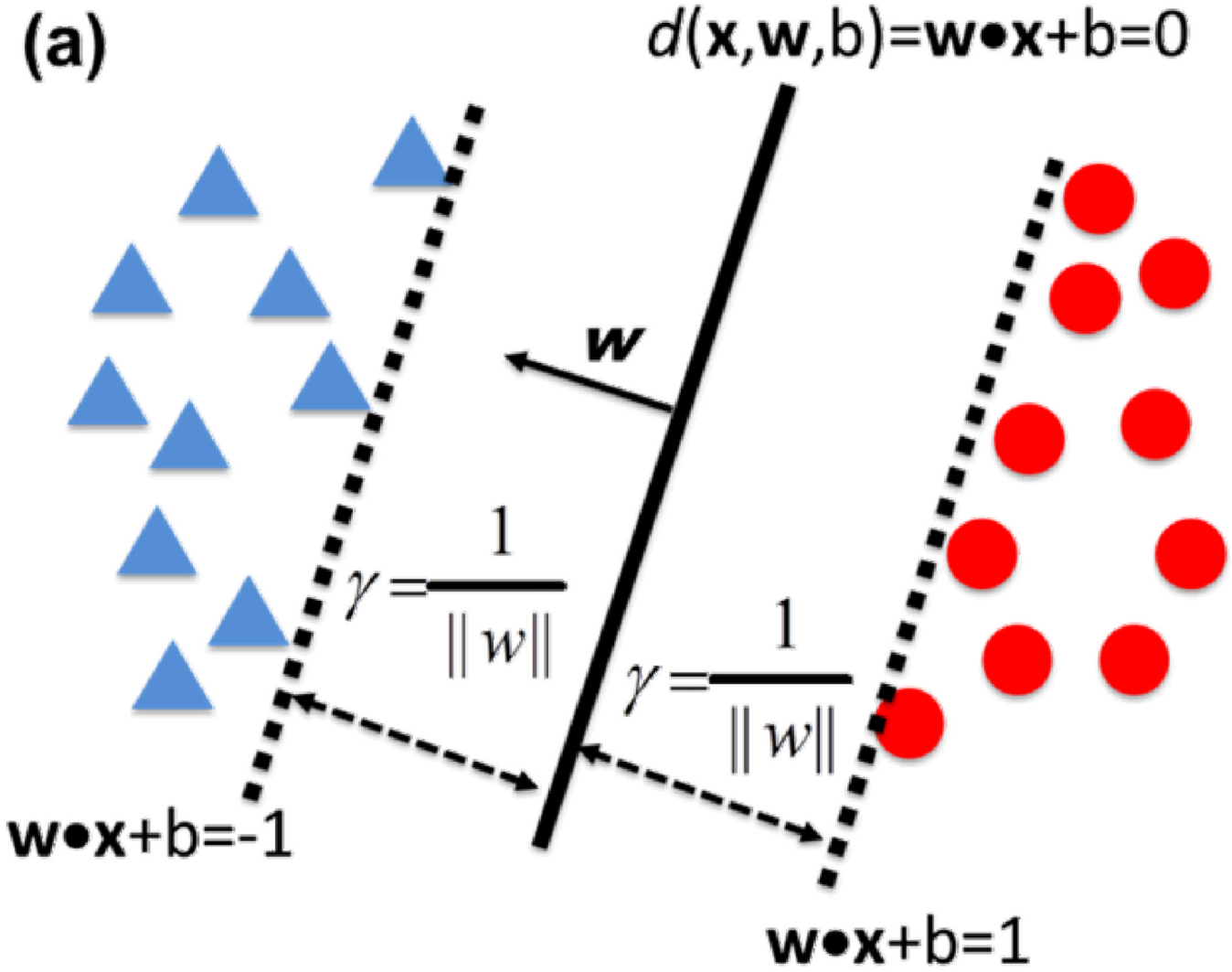

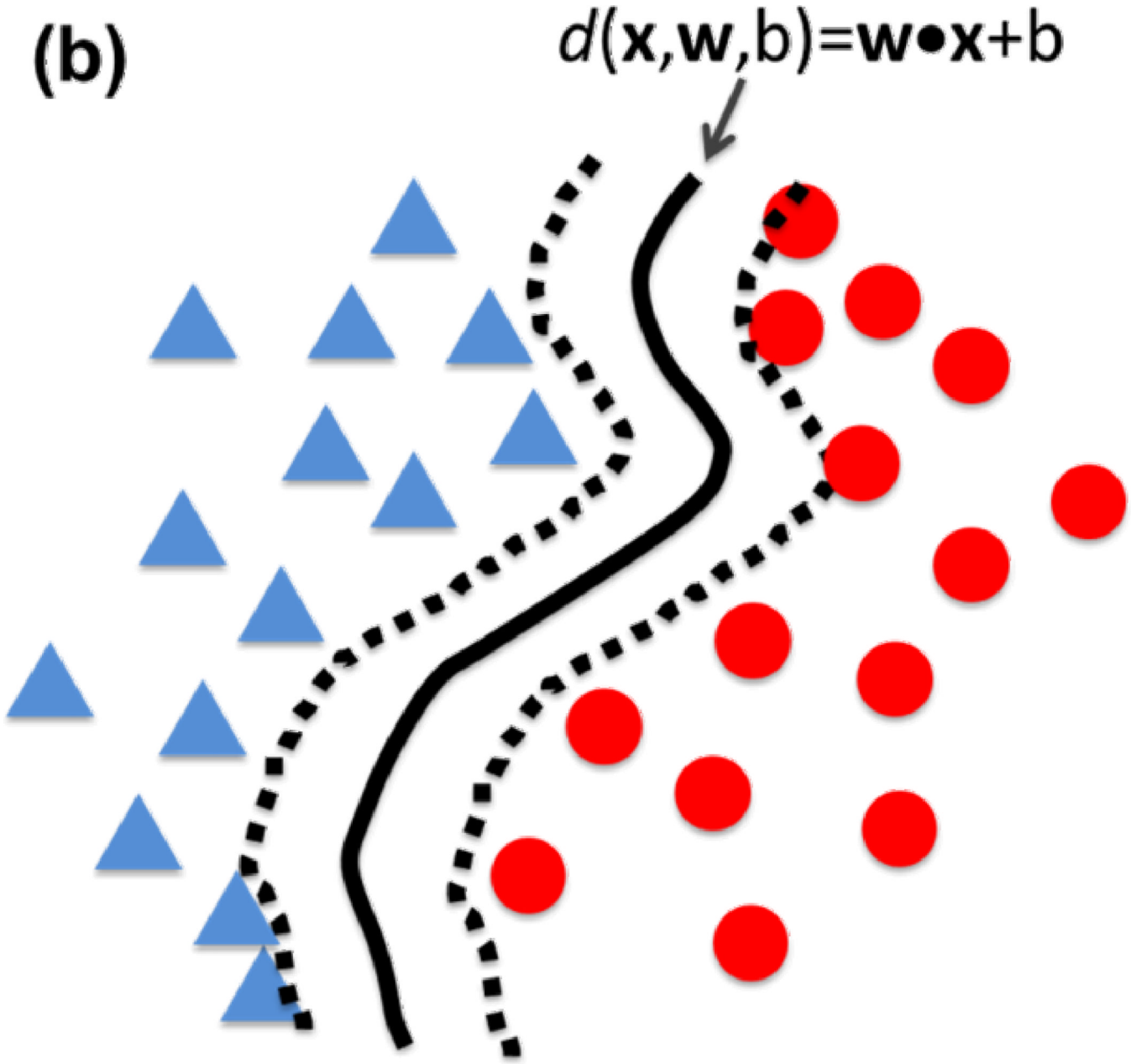

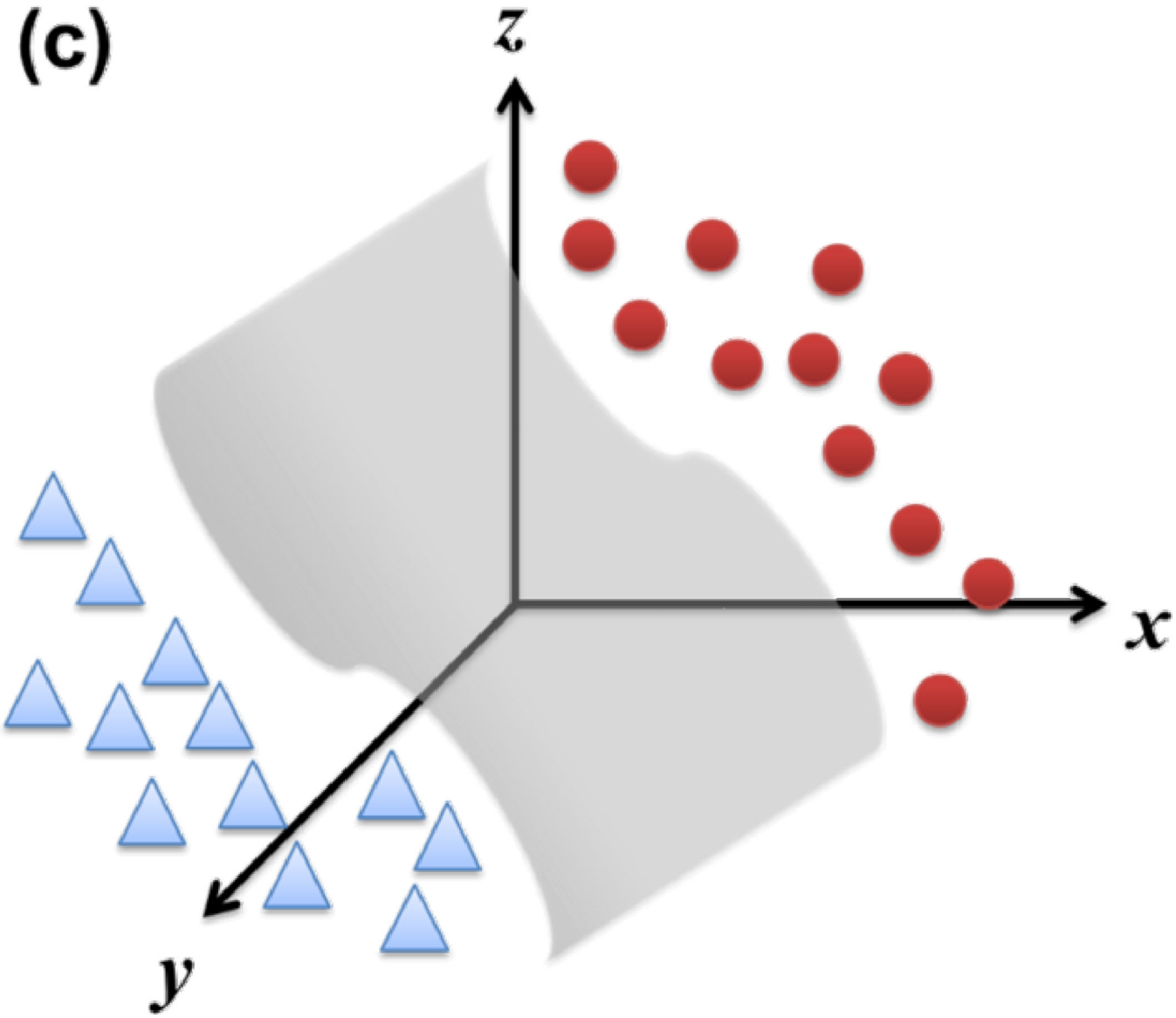

Figure 2.

(a) A hyperplane formed by SVMs for a linear classification. A filled red circle represents type I and a filled blue triangle represents type II. The thick line is the optimal hyperplane for classification, with w being the normal vector of hyperplane. Two dashed lines are the margins with a distance, γ, from the hyperplane. The condition $\gamma = 1/\|w\|$ is required to achieve functional margin for the canonical hyperplane. (b) A nonlinear hyperplane formed by SVMs with a nonlinear kernel function. (c) A nonlinear hyperplane in 3-dimensional space represented the multi-parameter analysis using SVMs.

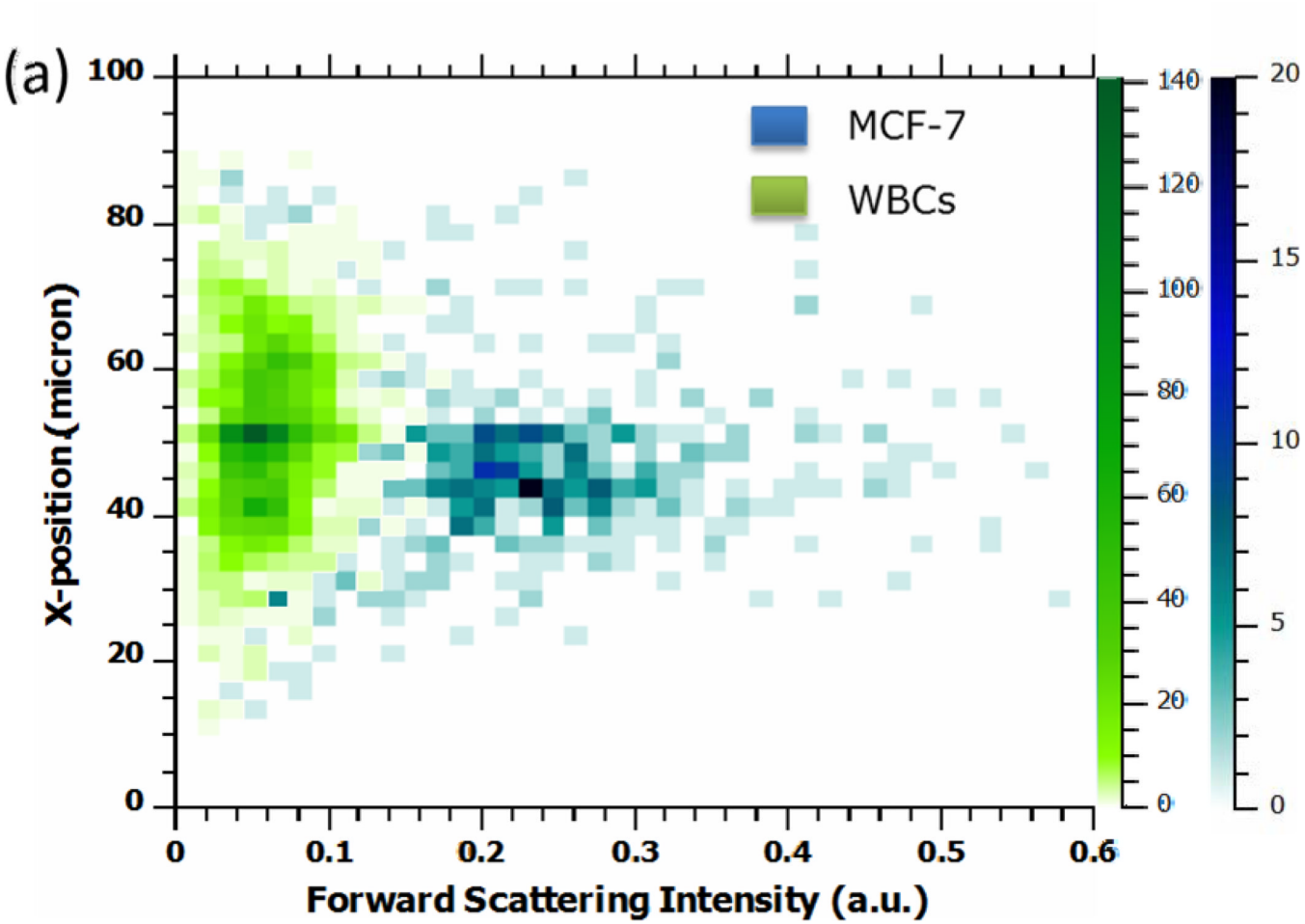

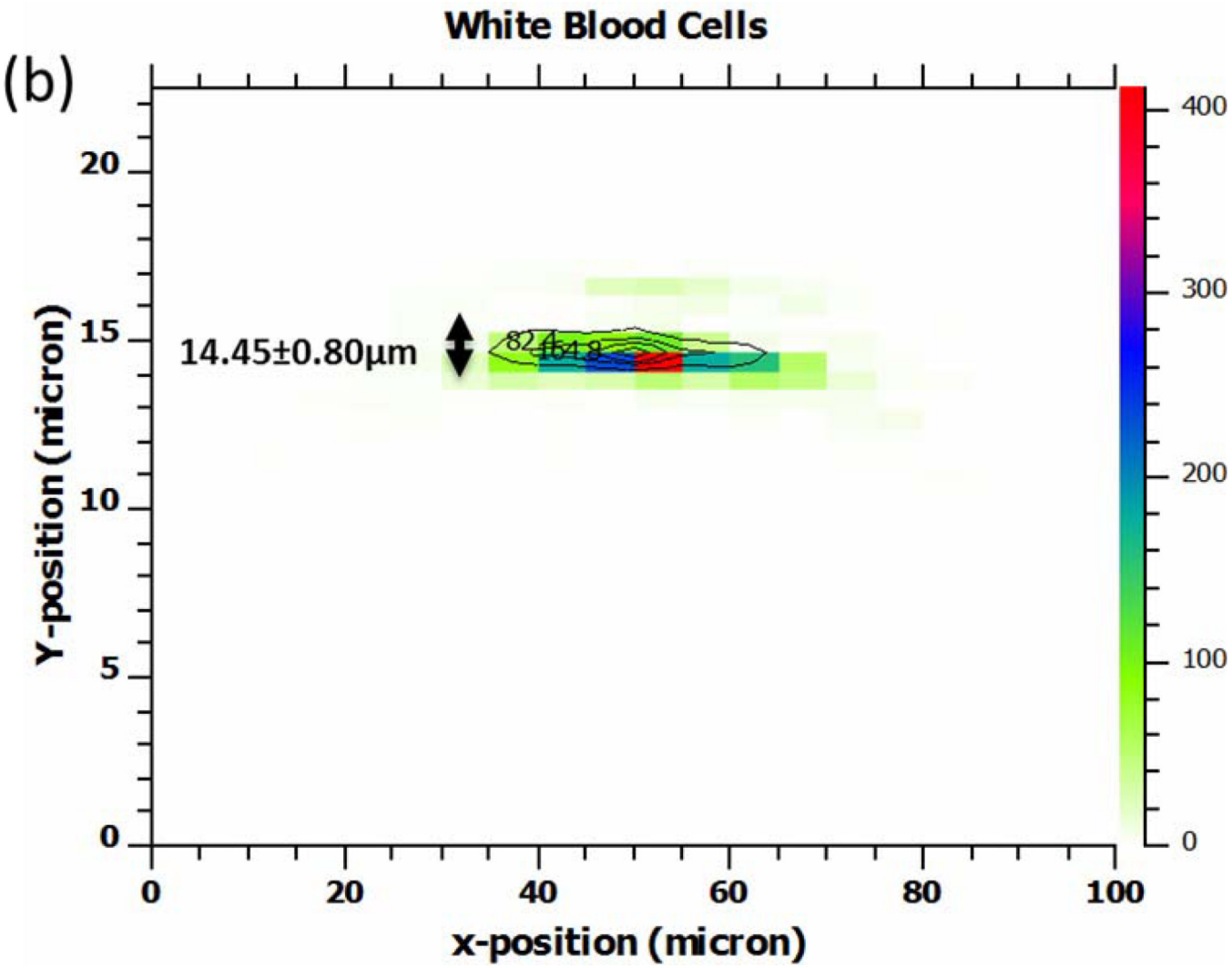

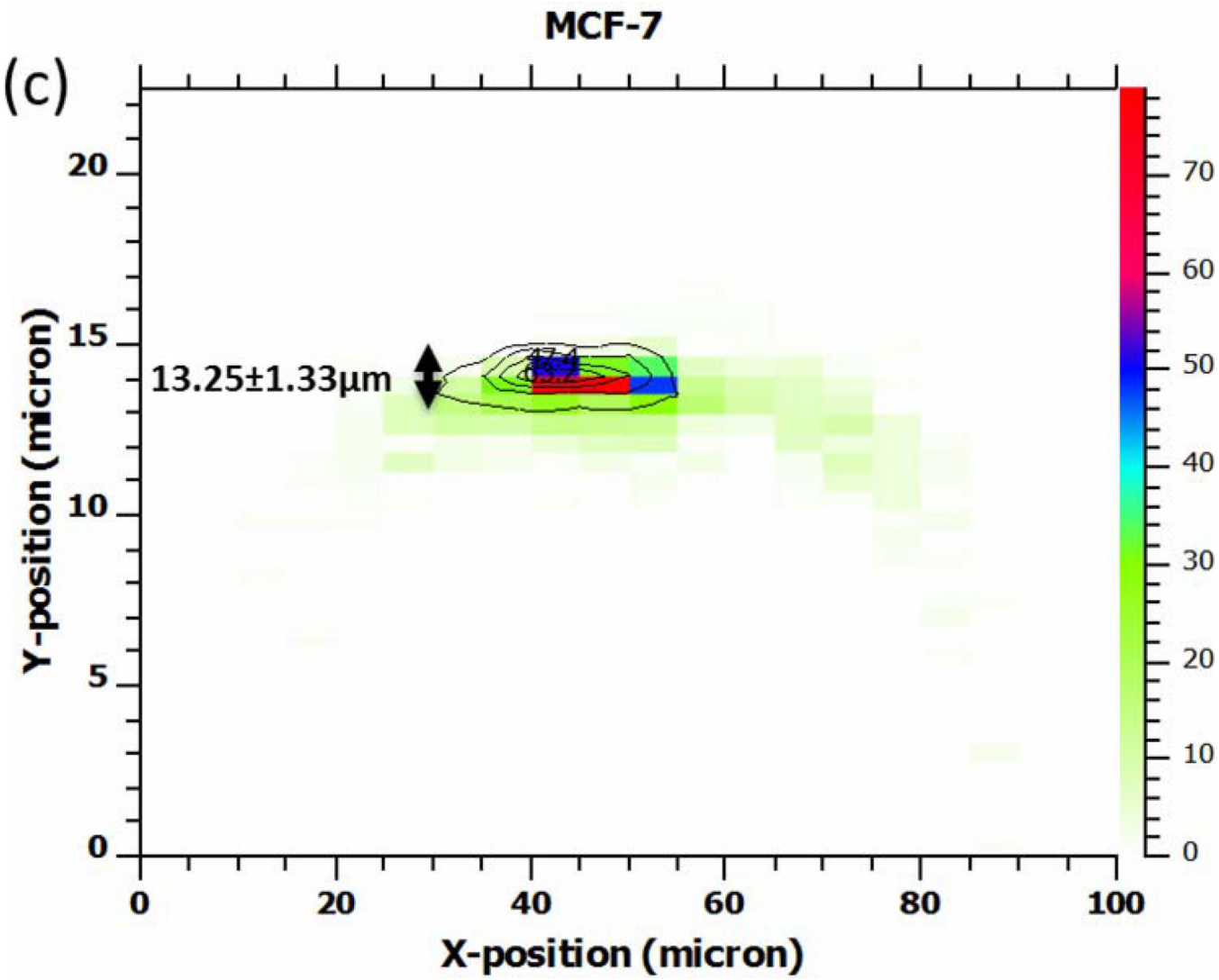

Figure 3.

(a) The superimposed contour plot of *x*-axis position versus forward scattering intensity for MCF-7 cells and white blood cells. The flow rate is at 75μL/min. (b) and (c) The spatial distribution contour plots of white blood cells and MCF-7 cells on the cross section of the half microchannel, respectively. Color bars in each figure represent the density of cell distribution.

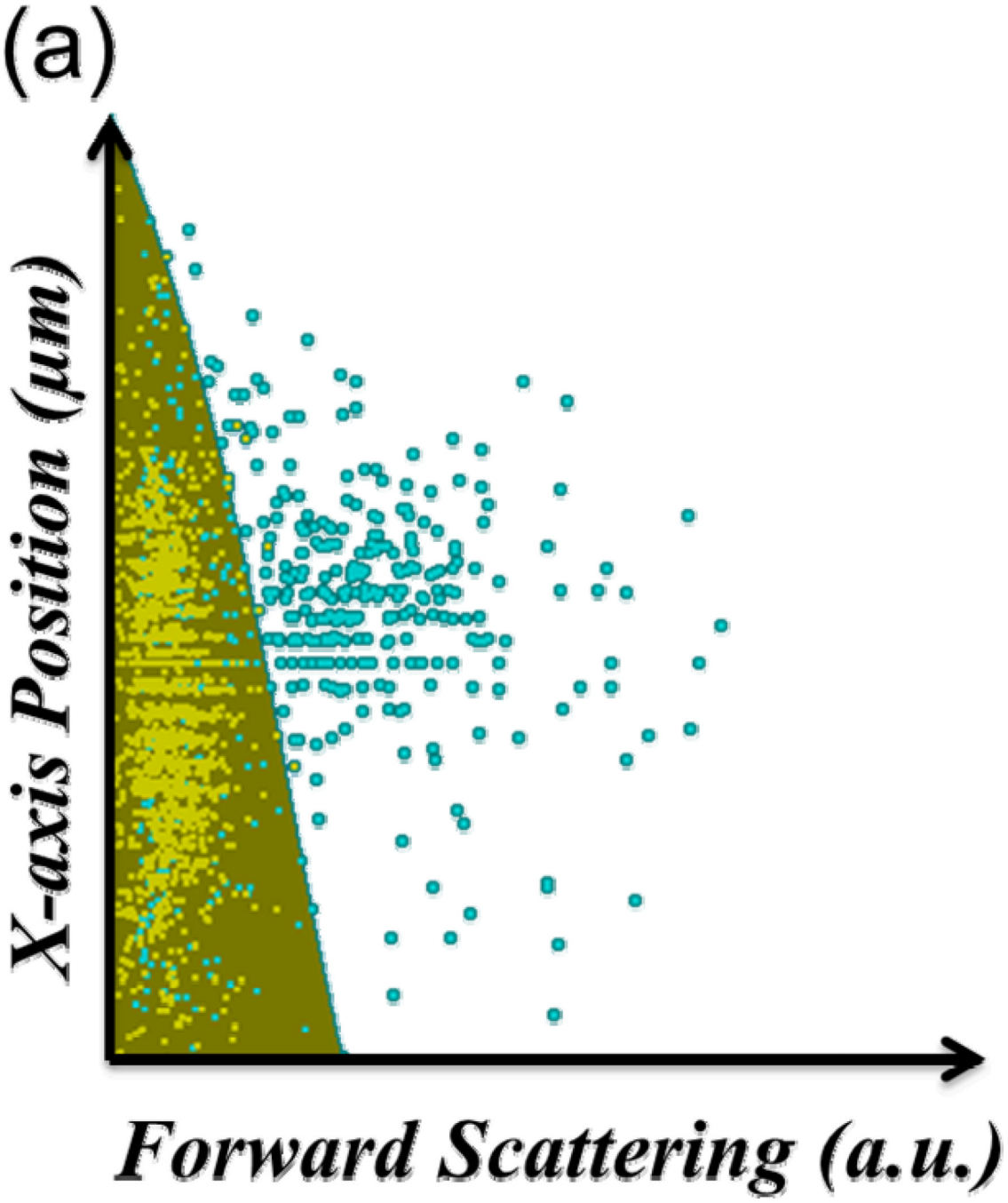

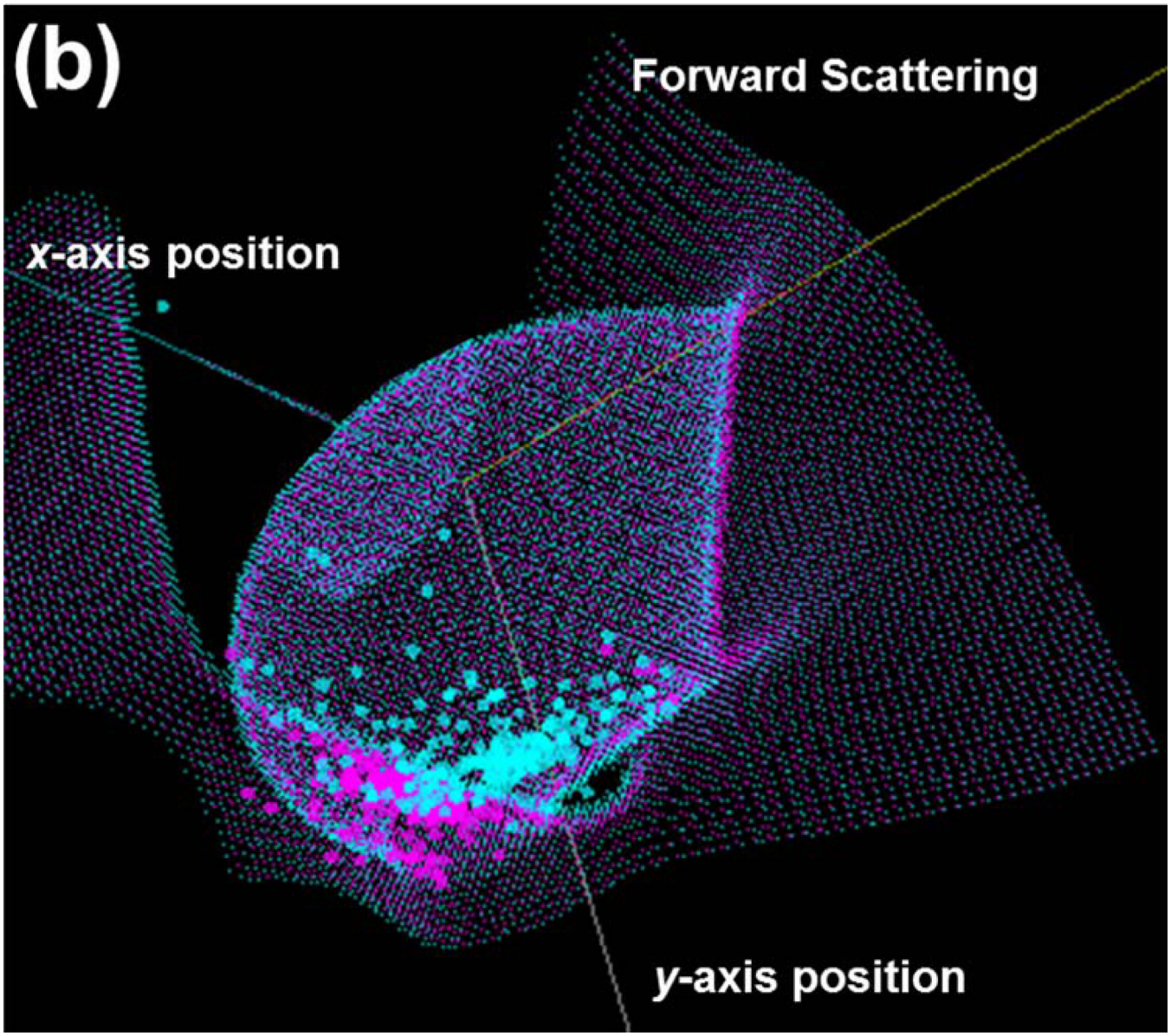

Figure 4.

(a) The hyperplane created by SVMs for 2-parameter cell classification, using forward scattering signals and position of cells along the *x*-axis. (b) The hyperplane created by SVMs for 3-parameter cell classification with the information of cell positions along *x*- and *y*-axes and the forward scattering intensity. This nonlinear hyperplane in 3-dimensional space allows multi-parameter analysis to achieve higher accuracy for cell classification.

Table 1

Summary of support vector machines for different dimensional analysis

Parameter	Trail	TP	TN	FP	FN	Accuracy	Sensitivity	Specificity
FS	I	156	762	12	124	87.09%	55.71%	98.45%
	II	169	770	4	114	88.83%	59.72%	99.48%
	III	155	773	1	126	87.96%	55.16%	99.87%
FS,X	I	161	761	13	119	87.48%	57.50%	98.32%
	II	164	773	2	118	88.56%	58.16%	99.74%
	III	179	754	22	100	88.65%	64.15%	97.16%
FS,X,Y	I	189	762	13	90	90.22%	67.74%	98.32%
	II	243	750	24	40	93.95%	85.87%	96.90%
	III	227	762	13	53	93.74%	81.07%	98.32%